9D.2 QUANTIFICATION OF SHEAR-RELATIVE PRECIPITATION ASYMMETRIES OF TROPICAL CYCLONES IN DIFFERENT INTENSITY CHANGE STAGES

Yongxian Pei* and Haiyan Jiang
Department of Earth and Environment, Florida International University, Miami, Florida

1. Introduction

Previous studies (Lonfat et al. 2004; Chen et al. 2006) have demonstrated that the Fourier wavenumber decomposition method is a very useful tool to quantify Tropical Cyclone (TC) precipitation asymmetries. These studies analyzed three years of Tropical Rainfall Measuring Mission (TRMM) rainfall data and showed the effects of storm motion and vertical wind shear on wavenumber-1 rainfall asymmetry across a range of intensities. In response to the challenge in forecasting Rapid Intensification (RI), Kieper and Jiang (2012) have shown that a symmetric precipitative ring feature in the microwave satellite image is an early indicator of RI. The unique contribution of this work towards understanding intensity change is to relate the rate of change to the degree of precipitation asymmetry using the Fourier decomposition method.

2. Data and Method

The dataset for this study consists of 14 years (1998 to 2011) of global TC overpasses from the TRMM Tropical Cyclone Precipitation Feature (TCPF) database (Jiang et al. 2011); intensity must be between tropical storm and category-2 strength (total sample is 1, 786 overpasses; Table 1). The storm centers interpolated from the best track were manually re-centered previously based on TMI 37-GHz color composite image. The rainfall estimates are from version 7 of the TRMM microwave imager (TMI) 2A12 algorithm (Kummerow et al. 1996, 2001). Environmental conditions for each overpasses are included in the dataset including the sea surface temperature (SST), the total precipitable water (TPW), and the vertical wind shear. Following Zagrodnik and Jiang (2014) these environmental criteria are applied to further subset the overpasses of interest.

Overpasses are divided into five intensity change categories (Zagrodnik and Jiang 2014): weakening (W), neutral (N), and slowly intensifying (SI), while RI is divided into two sub-categories, RI initial (RI INI) and RI continuing (RI CON).

For each grid cell (10x10 km^2) the precipitation occurrence is computed as the number of overpasses that are raining (rain rate, R ≥ 0.5 mm hr^{-1}) divided by the total number of overpasses in the sample. For the purpose of identifying statistical significance between different intensity change categories, this percentage occurrence is also computed for each shear-rotated quadrant from each case.

Similar to Lonfat et al. (2004), to quantify rainfall asymmetry, the Fourier decomposition is applied to the rainrate in 10-km wide annuli from the center. In each annulus, the Fourier coefficients are computed using (Stull 1987):

$$a_n = \frac{1}{N}\sum_{k=0}^{N-1} R(k)\cos(2\pi nk / N) \quad (1)$$

$$b_n = -\frac{1}{N}\sum_{k=0}^{N-1} R(k)\sin(2\pi nk / N) \quad (2)$$

where R(k) is the rain rate, n is the wavenumber, N is the total number of points (360) being analyzed in each annuli, and k is the index of each point. According to Zhu (et al. 2013), the total energy spectrum, as well as the contribution by each wavenumber, is computed from the above Fourier coefficients.

The dominant asymmetries are quantified using the sum of the wavenumber 1 through 6 amplitude divided by the mean rain rate over the entire annulus. The spatial structure of the dominant-order asymmetry (M) can be represented by,

$$M = \frac{\sum_{DW} a_n \cos(2\pi nk / N) - b_n \sin(2\pi nk / N)}{\overline{R}} \quad (3)$$

where DW are "dominant wavenumbers" (for example, wavenumber n equals to 1 through 6), and $\overline{R}$ is the mean rain rate calculated over the entire annulus.

3. Results

a) *Precipitation Distribution*

*Corresponding author address: Yongxian Pei, Dept. of Earth and Environment, Florida International University, Miami, FL 33199. Email: ypei002@fiu.edu

Fig. 1 shows the percentage occurrence of R ≥ 0.5 mm hr^{-1} for each intensity change category, oriented with respect to shear. The area of at least 80% occurrence progressively increases as intensity change rate of storms increase from W to N to SI to RI INI to RI CON. Compared to SI cases (occurrence less UR), the RI composite shows greater symmetry as the percent occurrence exceeds 80% in all quadrants, with the most prominent increase occurring UR. Within the RI composite itself, between RI INI (complete ring of 70% occurrence) and RI CON (of 90%), the occurrence also increases UR. The RI INI storms have more frequent precipitation UR than SI storms. Although the increase is not as great in this comparison as the other quadrants (Table 2), the very fact that all quadrants, including UR, are increasing suggests an important change in the distribution (area) of precipitation during intensification, and generally indicates that upshear rainfall plays an important role in TC RI. In Table 5, the total mean absolute difference (sum of all individual differences for each quadrant pair, e.g., DL-UR) in the occurrence during RI INI is significantly smaller than SI storms, which means that at RI INI storms are *more symmetric* than SI storms. The degree of symmetry increases even more substantially as RI continues (RI CON) as the total mean frequency difference is only 17% between RI INI and SI, compared with the difference between RI CON and RI that is 44.2%. Overall, the total absolute mean differences of percentage occurrence shows a decreasing order (increasingly symmetric) from W to N to SI to RI INI to RI CON (Table 3).

b) Fourier Asymmetry Composite

Now using the Fourier transform method, Fig. 2 also supports the conclusion that RI CON stage (and generally the entire RI period) the most symmetric given that the maximum wavenumber 1-6 normalized precipitation asymmetries are the smallest, while W, given it has the largest maximum, is the most asymmetric . During the RI INI stage storms appear to have two maxima (DL and DR), which suggests that the wavenumber 1 contributes less to the total perturbation in RI INI storms. One unique result from this methodology is that RI INI storms are less symmetric than SI storms.

4. Conclusion

The results show that upshear right rainfall coverage is important towards the initiation of RI. RI storms are generally more symmetric than non-RI storms. However at RI INI, storms are not as symmetric as the RI CON stage. Compared to SI storms, the precipitation occurrence of the RI INI stage in each quadrant is increasing, however the precipitation of UR is not increasing as fast as other quadrants, which at least in the Fourier transform method, leads to a more asymmetric precipitation distribution. This is a potentially distinguishing characteristic of RI INI; and future work will examine this result further.

References

Chen, S. S., J. A. Knaff, F. D. Marks, 2006: Effects of Vertical Wind Shear and Storm Motion on Tropical Cyclone Rainfall Asymmetries Deduced from TRMM. *Mon. Wea. Rev.*, **134**, 3190–3208.

Jiang, H., C. Liu, and E. J. Zipser, 2011: A TRMM-based tropical cyclone cloud and precipitation feature database. *J. Appl. Meteor. Climatol.* **50**,1255-1274.

Kieper, M. E., and H. Jiang, 2012: Predicting tropical cyclone rapid intensification using the 37GHz ring pattern identified from passive microwave measurements. Geophys. Res. Lett., 39, L13804, dio: 10.1029/2012GL052115.

Lonfat, M., F. D. Marks, and S. S. Chen, 2004: Precipitation distribution in tropical cyclones using the tropical rainfall measuring mission (TRMM) microwave imager: A global perspective. *Mon. Wea. Rev.*, **132**, 1645-1660.

Tao, C and H. Jiang, 2015: Distributions of Shallow to Very Deep Precipitation–Convection in Rapidly Intensifying Tropical Cyclones. *J. Climate*, **28**, 8791–8824.

Zagrodnik, J. P. and H. Jiang, 2014: Rainfall, Convection, and Latent Heating Distributions in Rapidly Intensifying Tropical Cyclones. *J. Atmos. Sci.*, **71**, 2789–2809.

Zhu, P., Menelaou, K. and Zhu, Z. (2014), Impact of subgrid-scale vertical turbulent mixing on eyewall asymmetric structures and mesovortices of hurricanes. Q.J.R. Meteorol. Soc., **140**: 416–438. doi: 10.1002/qj.2147

Table1. The sample size of different intensity change categories. (The RI cases missing negative 24h intensity have been categorized as RI initial. The cases missing Vmax (-18) or Vmax (-12) but have Vmax (-24) and their Vmax (0) - Vmax (-24) ≥ 30 kt have been categorized as RI continuing.)

Category	Max. Wind Speed Range (kt)	# TMI overpasses
W	Vmax(+24) – Vmax(0) < -0kt	339
N	-10 ≤ Vmax(+24) – Vmax(0) < 10kt	685
SI	10 ≤ Vmax(+24) – Vmax(0) < 30kt	554
RI	Vmax(+24)-Vmax(0) ≥ 30 kt	208
RI Initial	Vmax(+24)-Vmax(0) ≥ 30 kt and Vmax(0,+6,+12) – Vmax(-24,-18,-12) < 30 kt	91
RI continuing	Vmax(+24)-Vmax(0) ≥ 30 kt and Vmax(0,+6,+12) – Vmax(-24,-18,-12) ≥ 30 kt	117

Table 2. 2A12 rainrate percentage occurrence mean in the area of radius less than 150 KM in different quadrants. 90% significant different denoted as *; 95% significant different denoted as **; 99% significant different denoted as ***; 99.9% significant different denoted as ****. Significant tests are between RI and SI; RI INI and SI; RI CON and RI INI.

		DL	DR	UL	UR	TOTAL
Rainrate ≥ 0.5 mm/hr	W	66.5	54.0	49.2	40.5	52.6
	N	67.5	55.0	51.6	43.6	54.5
	SI	73.9	67.1	60.2	56.8	64.6
	RI	82.6****	77.9****	73.7****	69.3****	75.8****
	RI_INI	80.0**	76.1***	68.6**	61.7	71.5****
	RI_CON	84.6	79.3	77.7**	75.2****	79.2***

Table 3. 2A12 rainrate percent occurrence mean difference between different quadrants for different types of precipitation in different categories. 90% significant different denoted as *; 95% significant different denoted as **; 99% significant different denoted as ***; 99.9% significant different denoted as ****. Significant tests are between RI and SI; RI INI and SI; RI CON and RI INI.

		DL-DR	DL-UR	DL-UL	DR-UR	DR-UL	UR-UL	TOTAL
Rainrate ≥ 0.5 mm/hr	W	27.52	42.51	30.14	28.35	33.75	25.67	187.9
	N	27.78	44.07	30.7	28.47	32.01	25.45	188.5
	SI	24.25	38.61	30.36	28.72	33.5	23.23	178.7
	RI	18.45****	28.31****	21.71****	22.03****	26.10****	20.24**	136.8****
	RI_INI	21.6	33.97	24.52**	26.19	31.36	24.05	161.7*
	RI_CON	16.00**	23.90***	19.53*	18.80***	22.01***	17.27***	117.5****

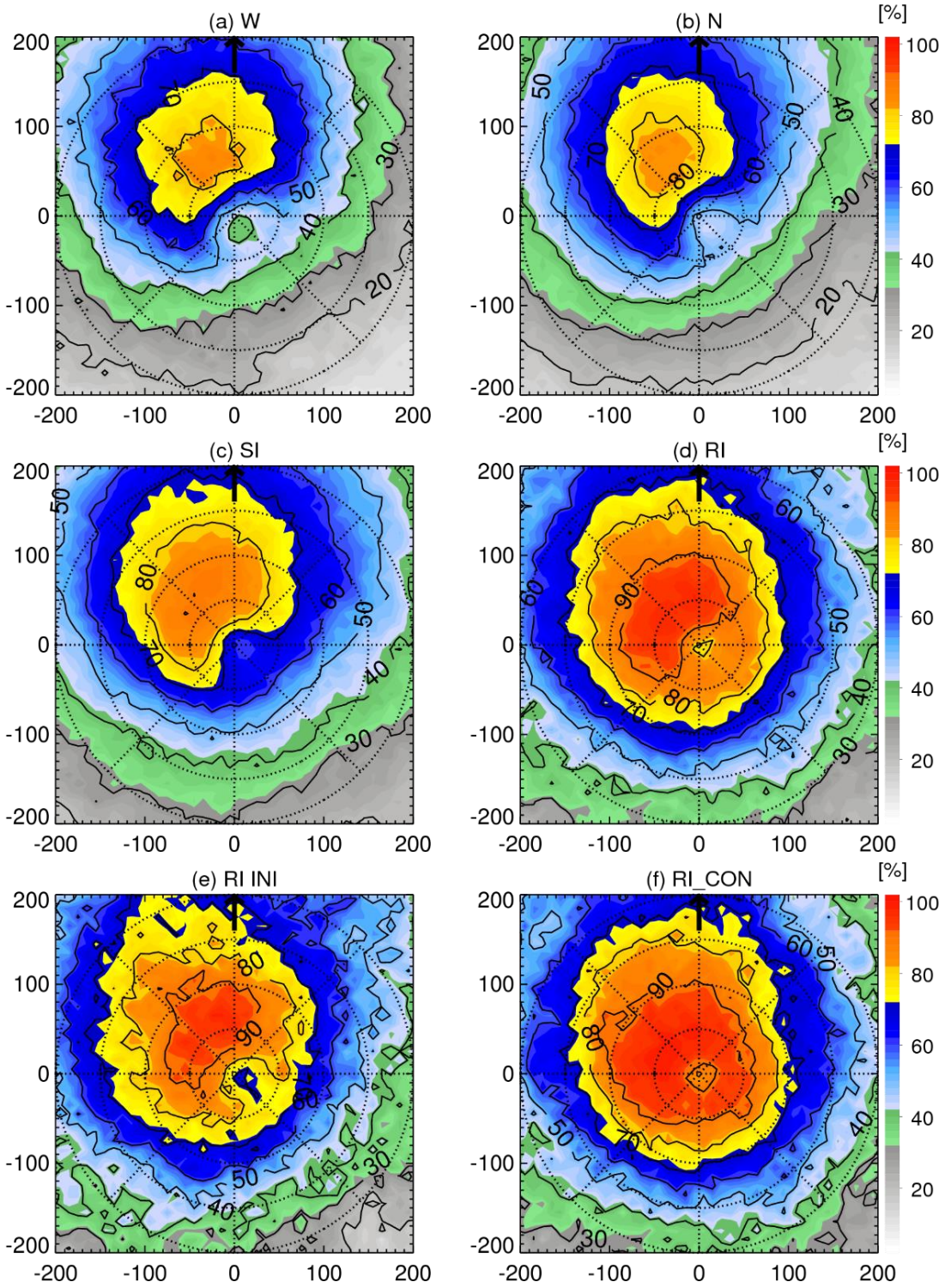

Figure1. Composite shear-relative distribution of the percentage of occurrence of 2A12 rain rate greater than or equal to 0.5 mm/hr for (a) RW, (b) SW, (c) N, (d) SI, (e) RI INI, (f) RI CON. [The shear-relative quadrants are downshear left (DL; upper left), downshear right (DR; upper right), upshear left (UL; lower left), and upshear right (UR; lower right).]

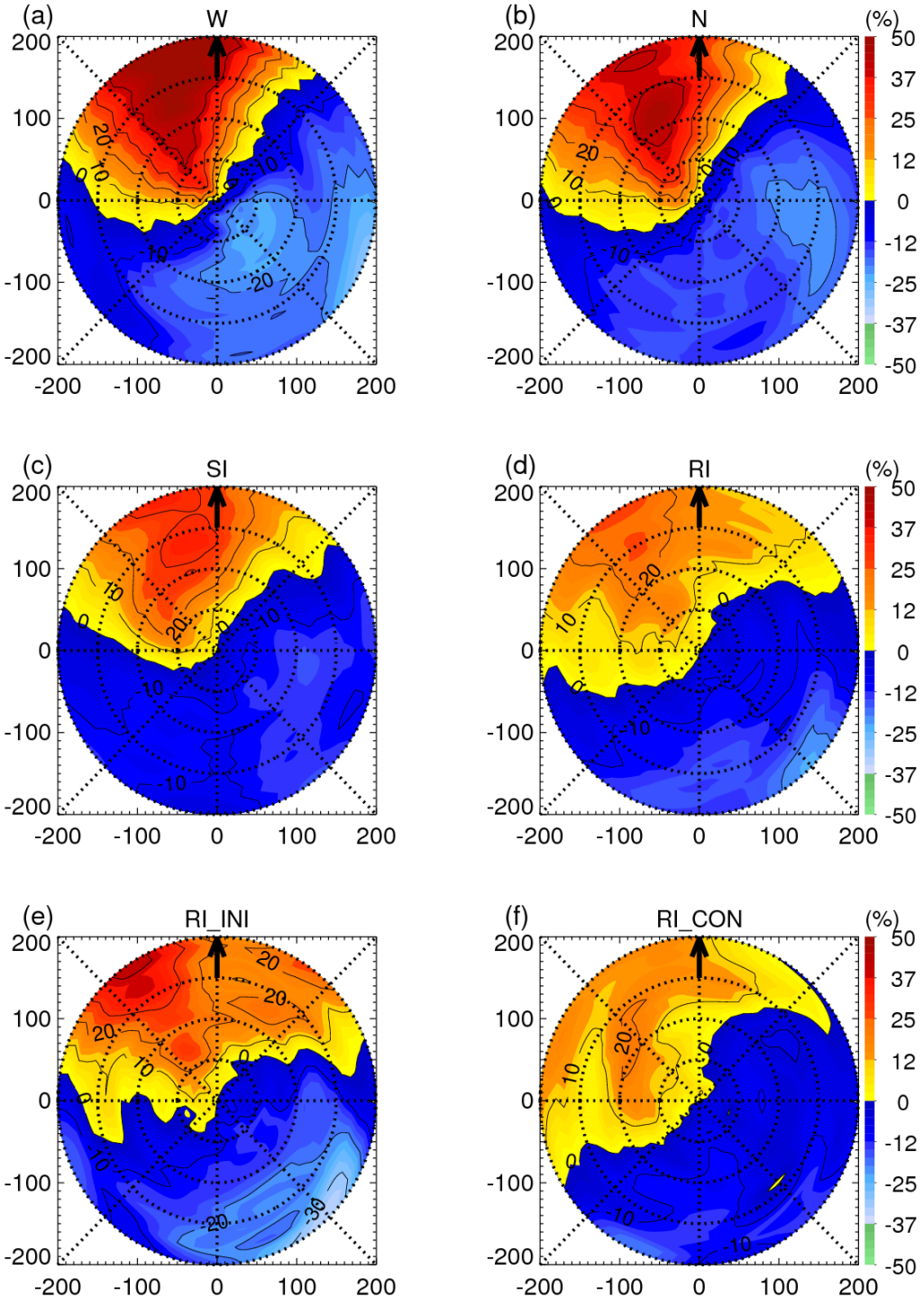

Figure 2. Composite shear-relative normalized wavenumber 1 through 6 Fourier asymmetry distribution of 2A12 rain rate ≥ 0.5 mm/hr for (a) W, (b) N, (c) SI, (d) RI, (e) RI INI, (f) RI CON